DØnote 4893-CONF

Search for Heavy Resonances Decaying into $Z + jet$ Final States in $p\bar{p}$ Collisions at $\sqrt{s} = 1.96$ TeV using the DØ Detector

The DØ Collaboration
URL http://www-d0.fnal.gov
(Dated: July 20, 2005)

A search has been carried out for heavy resonances decaying into $Z+jet$ final states in $p\bar{p}$ collisions at a center of mass energy of 1.96 TeV at the Tevatron using the DØ detector. No indication for the existence of such resonances has been found in a data sample corresponding to $\mathcal{L}_{\rm int} = 376 \pm 24$ pb^{-1} integrated luminosity. Mass values less than 520 GeV have been excluded at 95% CL.

Preliminary Results for Summer 2005 Conferences

Heavy resonances decaying into a quark and a gauge boson may signal the existence of excited quarks and thereby indicate a possible quark substructure [1]. Searches for excited quarks have been carried out in the past using di-jet [2–4], *photon+jet* and $W+jet$ [5] final states. In the present analysis we are searching for resonances in the $Z+jet$ channel, where the Z is detected via its $Z \longrightarrow e^+e^-$ decay mode. This signature is practically free of instrumental background. On the other hand it suffers from the low branching ratio of the $Z \longrightarrow e^+e^-$ decay channel. The high luminosity offered by the Tevatron in Run II makes it possible to present preliminary results for the first time on this final state.

The Run II DØ detector [6] consists of several layered subdetectors. For the present analysis the most relevant parts are the liquid-argon and uranium calorimeter [7] and the central-tracking system. The calorimeter has a central granularity of $\Delta\eta \times \Delta\phi = 0.1 \times 0.1$ where η is the pseudorapidity ($\eta = -\ln[\tan(\theta/2)]$), θ is the polar angle and ϕ is the azimuthal angle with respect to an axis defined by the proton beam. The central calorimeter (CC) covers pseudorapidities $|\eta|$ up to ≈ 1.1, and the two end calorimeters (EC) extend coverage to $|\eta| \approx 4.2$. The tracking system consists of a silicon microstrip tracker (SMT) and a central fiber tracker (CFT), both located within a 2 T superconducting solenoidal magnet, with designs optimized for tracking and vertexing at pseudorapidities $|\eta| < 3$ and $|\eta| < 2.5$, respectively.

The data used in this analysis were collected between April 2002 and August 2004, with an integrated luminosity of (376 ± 24) pb^{-1}. The selected events were required to pass at least one combination of single- or di-electron triggers. The efficiency of the trigger combination for events with two electrons was measured with data and was found to reach a plateau of $\varepsilon_{tr} = 0.982 \pm 0.011$ for electron pairs with the leading electron transverse momentum of $p_T^{e1} \geq 30$ GeV and the next-to-leading electron with $p_T^{e2} \geq 20$ GeV.

Final offline event selection was based on run quality, event properties, and electron and jet criteria. Events were required to have a reconstructed vertex with a longitudinal position within 50 cm of the detector center. Electrons were reconstructed from electromagnetic (EM) clusters in the calorimeter using a simple cone algorithm. The reconstructed electron candidates were required to be either in the region of $|\eta| \leq 1.2$ or in $1.5 < |\eta| \leq 2.5$. The highest-p_T electron candidate with $p_T^{e1} > 30$ GeV and the next to highest-p_T electron candidate with $p_T^{e2} > 25$ GeV in the event were used to reconstruct the Z boson candidate. The electron pair was required to have an invariant mass M_{ee} near the world average of the Z boson mass, $81 < M_{ee} < 101$ GeV.

To reduce background contamination, mainly from jets faking electrons, the EM clusters were required to pass three quality criteria based on shower profile: (i) the ratio of the EM energy to the total shower energy had to be greater than 0.9, (ii) the lateral and longitudinal shape of the energy cluster had to be consistent with those of an electron, and (iii) the electron had to be isolated from other energy deposits in the calorimeter with isolation fraction $f_{iso} < 0.15$. The isolation fraction is defined as $f_{iso} = [E(0.4) - E_{EM}(0.2)]/E_{EM}(0.2)$, where $E(R_{cone})$ and $E_{EM}(R_{cone})$ are the total and the EM energy, respectively, deposited within a cone of radius $R_{cone} = \sqrt{(\Delta\eta)^2 + (\Delta\phi)^2}$ centered around the electron. Additionally, at least one of the electrons was required to have a matching track with compatible momentum and direction to the EM cluster. A total of 24722 events passed these criteria.

Jets were reconstructed using the "Run II cone algorithm" [8] which combines particles within a cone of radius $R_{cone} = 0.5$. Spurious jets from isolated noisy calorimeter cells were eliminated by cuts on the jet shape and by requiring a minimum fraction of transverse energy of charged tracks associated to the jets. The transverse momentum of each jet was corrected (JES correction) for offsets due to the underlying event, multiple $p\bar{p}$ interactions and noise, for out-of-cone showering, and for detector energy response as determined from the missing transverse energy balance of photon–jets events. Jets were required to have $p_T > 10$ GeV and $|\eta| < 2.5$. Jets were eliminated if they overlapped with any of the reconstructed EM objects within a cone of $\Delta R = \sqrt{(\Delta\eta)^2 + (\Delta\phi)^2} = 0.4$. After the jet selection criteria, 4819 data events remained.

Jet losses were estimated using a Z+jet PYTHIA [9] Monte Carlo (MC) sample. Efficiencies for electron identification and track matching have been simulated using the same sample which has been passed through the complete reconstruction and analysis chain. In addition, a global *scale factor* has been applied to account for inefficiencies in data reconstruction not simulated by MC. This scale factor has been determined in the CC region as being 88% in Reference [10] where similar selection criteria have been used. By comparing the η distribution of the selected electrons in the data with those in the MC, this scale factor has been reduced to 83% when including the EC region.

In Fig. 1 the distribution of the invariant mass, M_{ee}, of the two selected electrons is shown, along with the simulated MC events using PYTHIA. In producing the latter smearing of the EM and hadronic jet energy has been applied in order to account for calorimeter effects which were not properly simulated. One can observe a very clean, almost background free Z signal which is described faithfully with the MC.

We have estimated two kinds of instrumental background where hadronic jets are misreconstructed as EM jets and mimic Z events. One type comes from genuine QCD events where both of the EM objects are in fact hadronic jets. The other source of background are $W \longrightarrow e\nu + j$ events where the hadronic jet associated to the W fakes an electron. The M_{ee} distribution of the QCD background has been parametrized as $f_{QCD} = a \cdot \mathrm{e}^{-dM_{ee}}$ and the parameter d has been obtained from a fit of data events where the shower shape criteria have been inverted and neither of the

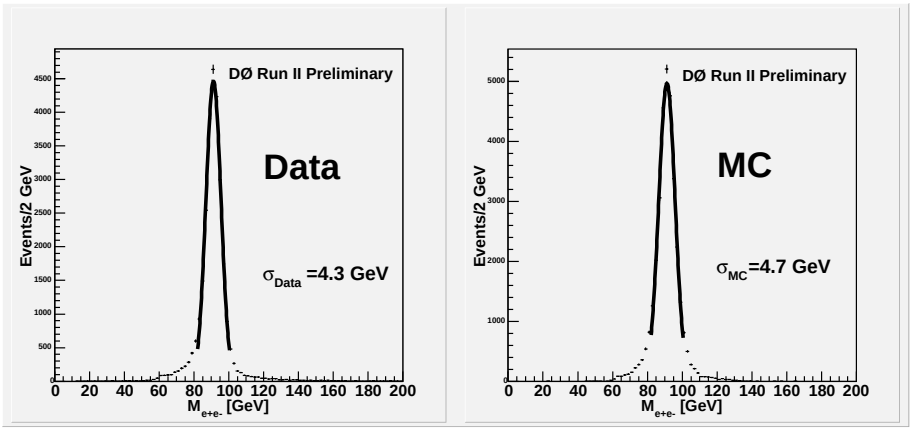

FIG. 1: The invariant mass distribution of the two selected electrons in the event: data - left and MC - right. A gaussian fit is performed around the Z peak which indicates that the widths of data and MC are of similar magnitude.

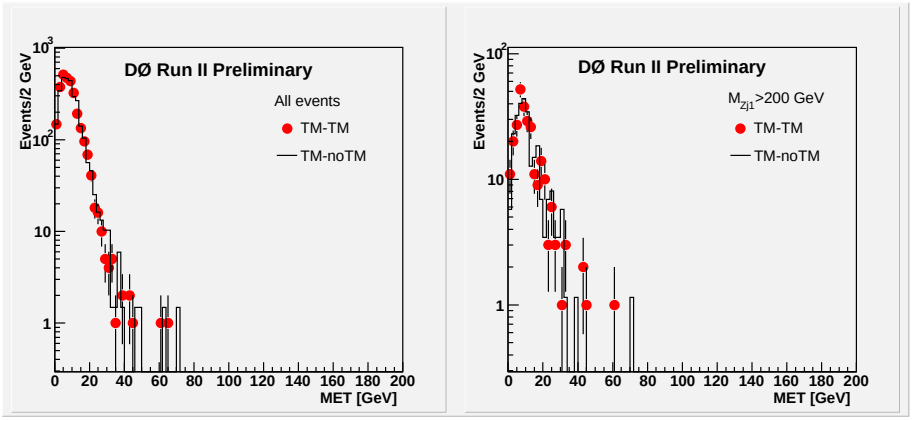

FIG. 2: MET distribution of events where only one electron has a matched track (solid histogram), and that of those where both electrons have a matched track (red dots). The two histograms are normalized to the same area. Left: all events, right: events with $M_{Zj1} > 200$ GeV.

EM objects had matched tracks. Assuming that the MC simulation describes correctly the Drell-Yan production of the e^+e^- pairs, the parameter a has been fitted using the difference of the data and MC events (*c.f.* Fig. 1) in the sidebands of the resonance: $60 < M_{ee} < 70$ GeV and $110 < M_{ee} < 130$ GeV. From the obtained value we have derived the amount of the QCD background as being $(0.74 \pm 0.02)\%$ under the Z peak. The $W \longrightarrow e\nu + j$ background, characterized by large missing transverse energy (MET), should appear in the data sample where only one of the EM objects has a matched track. In Fig. 2 a comparison is shown of the MET distributions of events where only one electron has a matched track with those where both of them do have a matched track. Since these distributions are similar, one can conclude that this type of background is small.

We consider the signal as a spin 1/2 resonance produced in quark-gluon fusion following the model of Reference [1] and implemented in PYTHIA. The corresponding Feynman diagram is depicted in Fig. 3. This reaction, where the resonance is produced in SM gauge interaction, is the dominant one but it is by far not the only possible way an excited quark can be produced. The compositeness scale Λ is taken to be the mass of the resonance and all form factors involved are set to unity. These conditions determine the widths of the resonances which are smaller than the experimental resolution ($\sim$ 70 GeV at $M_{q*} = 500$ GeV). In the simulation we have used PDF from CTEQ5L [11]. Typical signal acceptance is $\sim$ 20 %. The invariant mass of the Z and the leading jet, M_{Zj1}, for an excited quark of mass $M_{q*} = 500$ GeV is shown in Fig. 4.

The main background to the signal is inclusive Z boson production in the Standard Model (SM). We have generated 100 000 events in the entire region of M_{Zj1} by PYTHIA using the so-called $2 \longrightarrow 1$ process. In order to enhance the statistics in events of high M_{Zj1}, the region of interest of the present search, we have in addition generated PYTHIA events including 2nd order matrix elements ($2 \longrightarrow 2$ process). In order to avoid collinear divergences a minimum value of $p_{Tp} = 30$ GeV was used for the transverse momentum of the parton in the $2 \longrightarrow 2$ collision. Four samples

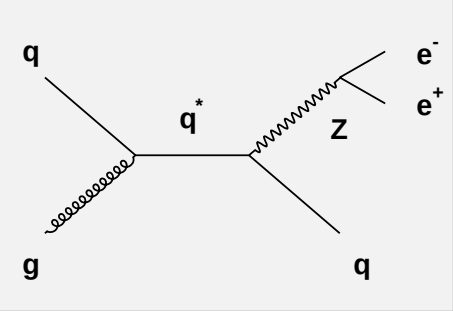

FIG. 3: Feynman diagram of the production of the excited quark considered in the present search.

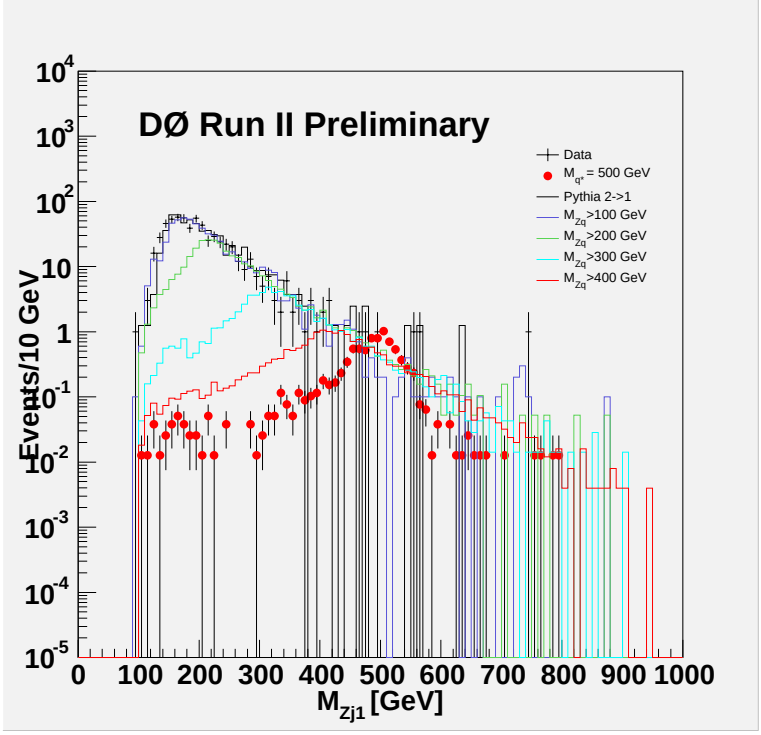

FIG. 4: Invariant mass distribution of the Z and of the leading jet, M_{Zj1} for the case of $p_{TZ} > 50$ GeV: Data - horizontal lines with error bars; PYTHIA $2 \longrightarrow 1$ - black histogram; PYTHIA $2 \longrightarrow 2$ - colored histograms with various M_{Zq} thresholds: 100 GeV - magenta, 200 GeV - green, 300 GeV - azure, 400 GeV - red; the resonance of mass 500 GeV - red dots. SM backgrounds are normalized to data. All $2 \longrightarrow 2$ processes have a common normalization factor determined for the $M_{Zq} = 100$ GeV threshold. The resonance is normalized to the total integrated luminosity.

with different thresholds of M_{Zq} =100, 200, 300 and 400 were simulated, where M_{Zq} is the invariant mass of the Z and the parton in the final state. Each sample consisted of about 25 000 events. All MC events were processed through the full detector simulation. The $2 \longrightarrow 1$ process describes the data well for $M_{Zj1} < 300$ GeV whereas the $2 \longrightarrow 2$ processes agree well with the data for $M_{Zj1} > 150$ GeV. The transverse momentum distribution of the Z also agrees well with the data for $p_{TZ} > 50$ GeV. In the following we use only the $2 \longrightarrow 2$ process for simulation of the SM background with an M_{Zq} threshold chosen according to the M_{Zj1} region to be investigated (see Table II). The M_{Zj1} distribution for data and for the PYTHIA MC samples is shown in Fig. 4.

The background shape has also been tested with the ALPGEN generator [12]. For this purpose 37750, 10000 and 21700 events have been generated for $Z + 0j$, $Z + 1j$ and $Z + 2j$ samples, respectively. The shapes obtained by the PYTHIA and ALPGEN generators agree within statistical fluctuation.

Since no significant peak can be observed in the M_{Zj1} data distribution (*c.f.* Fig. 4) we proceed to determine the upper limit of the production cross section of the excited quark as a function of its mass. We make use of the fact that in the p_{TZ} *vs* M_{Zj1} plane the events from the resonance are concentrated for M_{Zj1} around the mass value and

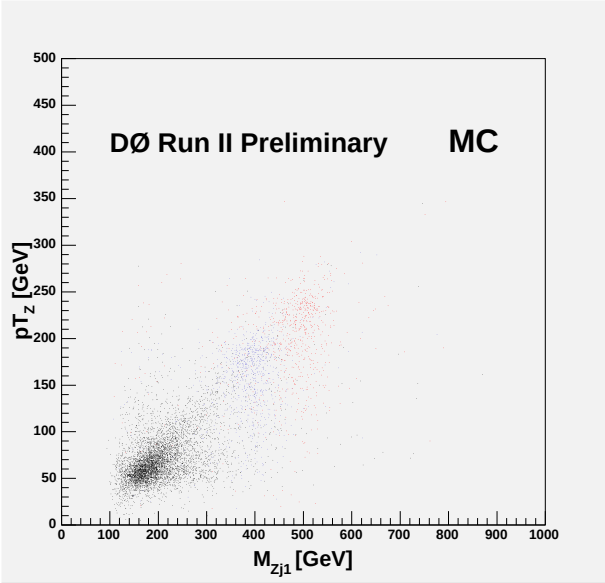

FIG. 5: p_{TZ} *vs* M_{Zj1} for SM background (black) and resonances with masses of 400 GeV (blue) and of 500 GeV (red) points.

TABLE I: Central values and RMS of the M_{Zj1} and p_{TZ} distributions of the excited quarks of different masses.

Mass (GeV)	M^c_{Zj1} (GeV)	M^{rms}_{Zj1} (GeV)	p^c_{TZ} (GeV)	p^{rms}_{TZ} (GeV)
300	295.0	56.6	122.5	34.5
400	395.0	67.5	187.5	42.9
500	505.0	89.2	232.5	50.9
600	595.0	99.3	262.5	64.2
700	675.0	116.4	312.5	74.7

for p_{TZ} around about half of the mass value of the resonance, whereas the SM background does not exhibit a similar structure (*c.f.* Fig. 5). Hence we consider events around the central (peak) value of M^c_{Zj1} and of p^c_{TZ} of the resonance determined by the following condition:

$$\left(\frac{M_{Zj1} - M^c_{Zj1}}{M^{rms}_{Zj1}}\right)^2 + \left(\frac{p_{TZ} - p^c_{TZ}}{p^{rms}_{TZ}}\right)^2 = k^2 \tag{1}$$

where M^{rms}_{Zj1} and p^{rms}_{TZ} are the RMS values of the corresponding distributions of the resonance, and k is a cut value to be optimized.

The SM background has been normalized to the data in the $M_{Zj1} > 150$ GeV and $p_{TZ} > 50$ GeV region. Five different mass values for the excited quark have been considered which are displayed in Table I along with the corresponding values of M^c_{Zj1}, M^{rms}_{Zj1}, p^c_{TZ} and p^{rms}_{TZ}. At a given mass value we have varied k (*c.f.* Eq.(1)) between 0 and 3 in a step of 0.1. Based only on information from the signal and background simulation, for each k we have calculated σ^{ave}_{95}, the *average value* of the upper limit of the resonance production cross section at 95% confidence level (CL) using a Bayesian approach [13]. The calculation uses an algorithm described in Reference [14] and can be found on [15]. The optimum of k corresponds to the minimum value of σ^{ave}_{95}. At this minimum we have derived from the data σ_{95} the *measured value* of the upper limit of the resonance production cross section at 95% confidence level (CL) using the computer code [15].

The σ_{95} values are displayed in Table II for each mass of the excited quark along with the optimum of the cut parameter k. The relatively high (low) values of the parameter k at the resonance mass values of 400 (700) GeV are due to statistical fluctuation. Also shown are the acceptance of the resonance, the number of data and SM background events. In addition to the statistical error the uncertainty of the acceptance contains also the uncertainty on the trigger efficiency and on the scale factor. We have verified that the JES uncertainty has no impact on the uncertainty of the acceptance. The major part of the uncertainty on the SM background is the statistical error of the generated background events, to which we have added quadratically the same amount of error to take into account uncertainties in the model used. We have also added quadratically the statistical error of the normalization and a 5%

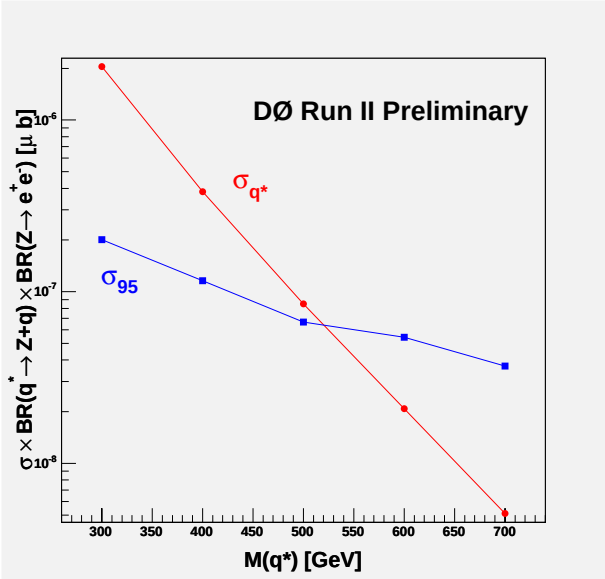

FIG. 6: Upper limit of the resonance cross sections at 95% confidence level (blue squares) along with the production cross section of the excited quarks times their decay branching fraction into $Z + jet$ and $Z \longrightarrow e^+e^-$ (red circles).

TABLE II: σ_{95} at the optimal value of the topological cut k.

Mass (GeV)	k	σ_{95} (pb)	σ_{95}^{ave} (pb)	Acceptance	SM background	Data	M_{Zq} threshold (GeV)
300	0.9	0.201	0.200	0.150 ± 0.010	41.59 ± 4.65	35	100
400	2.2	0.111	0.115	0.226 ± 0.013	35.66 ± 3.59	30	200
500	2.1	0.066	0.066	0.240 ± 0.014	10.94 ± 1.42	7	200
600	2.4	0.054	0.055	0.278 ± 0.014	7.06 ± 0.75	5	300
700	1.3	0.037	0.041	0.220 ± 0.011	0.71 ± 0.10	0	400

systematic uncertainty which accounts for fluctuations due to the choice of the region of the normalization. Finally, another 5% error has been added due to uncertainties in the JES. The σ_{95} values are also displayed in Fig. 6 along with the production cross section values of the excited quark as a function of its mass. The latter have been calculated using PYTHIA. One can conclude that mass values below 520 GeV are excluded by the present measurement in the framework of the model considered.

Acknowledgments

We thank the staffs at Fermilab and collaborating institutions, and acknowledge support from the Department of Energy and National Science Foundation (USA), Commissariat à l'Energie Atomique and CNRS/Institut National de Physique Nucléaire et de Physique des Particules (France), Ministry of Education and Science, Agency for Atomic Energy and RF President Grants Program (Russia), CAPES, CNPq, FAPERJ, FAPESP and FUNDUNESP (Brazil), Departments of Atomic Energy and Science and Technology (India), Colciencias (Colombia), CONACyT (Mexico), KRF (Korea), CONICET and UBACyT (Argentina), The Foundation for Fundamental Research on Matter (The Netherlands), PPARC (United Kingdom), Ministry of Education (Czech Republic), Natural Sciences and Engineering Research Council and WestGrid Project (Canada), BMBF (Germany), A.P. Sloan Foundation, Civilian Research and Development Foundation, Research Corporation, Texas Advanced Research Program, and the Alexander von Humboldt Foundation.

[1] U. Baur, M. Spira and P. Zerwas, Phys. Rev. D **42**, 8158 (1990).
[2] UA2 Collaboration, J. Alliti *et al.*, Nucl. Phys. B **400**, 3 (1993).

[3] CDF Collaboration, F. Abe *et al.*, Phys. Rev. D **55**, 5263 (1997).
[4] DØ Collaboration, Phys. Rev. D **69**, 111101(R) (2004).
[5] CDF Collaboration, F. Abe *et al.*, Phys. Rev. Lett. **72**, 3004 (1994).
[6] DØ Collaboration, V. Abasov *et al.*, "The Upgraded DØ Detector", in preparation fot submission to Nucl. Instrum. Methods Phys. Res. A, and T. LeCompte and H.T.Diehl, Ann. Rev. Nucl. Part. Sci. **50**, 71 (2000).
[7] DØ Collaboration, S. Abachi *et al.*, Nucl. Instrum. Methods Phys. Res. A**338**, 185 (1994).
[8] G.C. Blazey *et al.*, in *Proceedings of the Workshop: QCD and Weak Boson Physics in Run II*, edited by U. Baur, R.K. Ellis and D. Zeppenfeld, Batavia, Illinois (200) p. 47. See Section 3.5 for details.
[9] T. Sjöstrand, P. Edén, C. Friberg, L. Lönnblad, G. Miu, S. Mrenna and E. Norrbin, Computer Physics Commun. **135**, 238 (2001).
[10] DØ Collaboration, V.M. Abazov *et al.*, "Measurement of the Ratio of the $Z/\gamma^*(\longrightarrow e^+e^-)+ \geq n$ Jet Production Cross Section to the Total Inclusive $Z/\gamma^*(\longrightarrow e^+e^-)$ Cross Section in $p\bar{p}$ Collisions at $\sqrt{s} = 1.96$ TeV" DØ Note 4794-CONF, April 21, 2005.
[11] H. L. Lai, J. Huston, S. Kuhlmann, J. Morfin, F. Olness, J. F. Owens, J. Pumplin, W. K. Tung, Global QCD Analysis of Parton Structure of the Nucleon: CTEQ5 Parton Distributions hep-ph/9903282.
[12] M.L. Mangano, M. Moretti, F. Piccinini, R. Pittau, A. Polosa, hep-ph/0206293, JHEP 0307, 001 (2003),
M. L. Mangano, M. Moretti, R. Pittau, Nucl. Phys. **B539**, 215 (1999),
M.L. Mangano, M. Moretti, R. Pittau, Nucl. Phys. **B632**, 343 (2002).
[13] G. Landsberg, private communication
[14] I. Bertram *et al.*, "A Recipe for the Construction of Confidence Limits", DØ Note 3476.
[15] `http://www-d0.fnal.gov/~hobbs/limit_calc.html`